5. On the Coupled Motion of Steering and Rolling of a High-speed Container Ship

Kyoung-Ho SON*, *Member* and Kensaku NOMOTO**, *Member*

(*From J.S.N.A. Japan, Vol. 150, Dec. 1981*)

Summary

Yaw-sway-roll coupling motion of a ship is investigated on the basis of captive model tank tests. A single-screw, high-speed container ship has been chosen as a typical type for the study.

The smaller metacentric height naturally results in the heavier coupling of roll into yaw and sway, which affects manoeuvrability significantly: turning performance is improved by the coupling effect, and course-stability and quick response to steering are reduced. In short, the roll coupling lessens the hydrodynamic damping to yaw and sway acting upon the hull.

When an automatic course-keeping device is introduced, as is quite popular in modern navigation, another element of coupling is added: the rudder is activated in accordance with the yaw motion. This yaw-sway-roll-rudder coupling can become the cause of the heavy rolling often experienced on high-speed ships automatically steered in a seaway. We make use of a perturbation stability analysis of the problem to reveal the mechanics of the unstable character of the coupled motion of a ship. Introducing rate-control to the autopilot gives a remarkable stabilizing effect.

1. Introduction

In recent years the yaw-roll coupling has drawn an increasing amount of attention[1),2),3)]. This phenomenon becomes particularly significant when:

(1) A ship has rather a small metacentric height and thus she tends to heel over with steering.

(2) A ship is operating at high-speed where hydrodynamic heeling moment caused by yaw and sway becomes considerable.

These situations often occur for modern high-speed container carriers, RO-RO ships, and some kinds of swift naval vessels.

We take a single-screw, high-speed container ship as a typical type for the present study. On the basis of captive model tank tests with varying heel angles, a set of equations of yaw-sway-surge-roll coupled motion are derived. The equations are employed to predict the hard-over turning performance and zig-zag steering behaviour of the ship, taking into account the effect of roll motion. We also use of the same equations, together with another equation for rudder control, to investigate the mechanics of the instability of the yaw-sway-roll-rudder coupled motion. This instability can induce a self-exciting, heavy rolling coupled with a considerable yawing of the same frequency.

* University of Osaka, Graduate School, Dept. of Naval Architecture

** University of Osaka, Dept. of Naval Architecture, Professor

2. Equations of Motion

Fig. 1 shows the co-ordinate system to be used. Neglecting the effect of pitch and heave, we obtain the fundamental equations of surge,

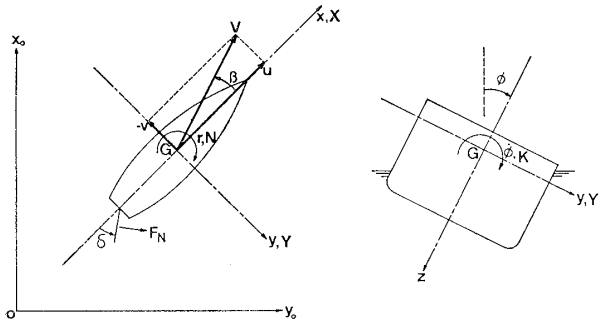

Fig. 1 Co-ordinate system

sway, yaw and roll coupled motion:

$$\left.\begin{aligned} &m(\dot{u}-vr)=(\text{all the surge force})\\ &m(\dot{v}+ur)=(\text{all the sway force})\\ &I_z\dot{r}=(\text{all the yaw moment})\\ &I_x\ddot{\phi}=(\text{all the roll moment}) \end{aligned}\right\} \quad (1)$$

where m denotes the ship's mass, and I_z and I_x her moment of inertia about the z and x axes, respectively.

According to the established procedure of dealing with hydro-inertial terms involved in the right-hand sides, and also introducing the static transverse stability moment included in the roll moment, Eqs. (1) becomes

$$\left.\begin{aligned} &(m+m_x)\dot{u}-(m+m_y)vr=X\\ &(m+m_y)\dot{v}+(m+m_x)ur\\ &\qquad +m_y\alpha_y\dot{r}-m_yl_y\ddot{\phi}=Y\\ &(I_z+J_z)\dot{r}+m_y\alpha_y\dot{v}=N-Yx_G\\ &(I_x+J_x)\ddot{\phi}-m_yl_y\dot{v}-m_xl_xur\\ &\qquad +\mathrm{WGM}\phi=K_0 \end{aligned}\right\} \quad (2)$$

where X and Y denote the hydrodynamic forces (ex. hydro-inertial forces) in the x and y directions respectively, N the hydrodynamic yaw moment about the midship, x_G the distance of C.G. in front of the midship, and K_0 the hydrodynamic roll moment about C.G. m_x, m_y, J_z and J_x denote the added mass and added moment of inertia in the x and y directions and about the z and x axes, respectively. α_y denotes the x-co-ordinates of the centre of m_y, and l_x and l_y the z-co-ordinates of the centres of m_x and m_y, respectively. The hydrodynamic forces and moments are written down using hydrodynamic derivatives as follows:

$$\left.\begin{aligned} X=&\frac{\rho}{2}L^2V^2\{X'(u')+(1-t)T'(J)+X'_{vr}v'r'\\ &+X'_{vv}v'^2+X'_{rr}r'^2+X'_{\phi\phi}\phi^2\\ &+c_{RX}F'_N\sin\delta\}\\ Y=&\frac{\rho}{2}L^2V^2\{Y'_vv'+Y'_rr'+Y'_{\dot{\phi}}\dot{\phi}'+Y'_\phi\phi\\ &+Y'_{vvv}v'^3+Y'_{rrr}r'^3+Y'_{vvr}v'^2r'\\ &+Y'_{vrr}v'r'^2+Y'_{vv\phi}v'^2\phi+Y'_{v\phi\phi}v'\phi^2\\ &+Y'_{rr\phi}r'^2\phi+Y'_{r\phi\phi}r'\phi^2\\ &+(1+a_H)F'_N\cos\delta\}\\ N=&\frac{\rho}{2}L^3V^2\{N'_vv'+N'_rr'+N'_{\dot{\phi}}\dot{\phi}'+N'_\phi\phi\\ &+N'_{vvv}v'^3+N'_{rrr}r'^3+N'_{vvr}v'^2r'\\ &+N'_{vrr}v'r'^2+N'_{vv\phi}v'^2\phi+N'_{v\phi\phi}v'\phi^2\\ &+N'_{rr\phi}r'^2\phi+N'_{r\phi\phi}r'\phi^2\\ &+(x'_R+a_Hx'_H)F'_N\cos\delta\}\\ K_0=&\frac{\rho}{2}L^3V^2\{K'_vv'+K'_rr'+K'_{\dot{\phi}}\dot{\phi}'+K'_\phi\phi\\ &+K'_{vvv}v'^3+K'_{rrr}r'^3+K'_{vvr}v'^2r'\\ &+K'_{vrr}v'r'^2+K'_{vv\phi}v'^2\phi+K'_{v\phi\phi}v'\phi^2\\ &+K'_{rr\phi}r'^2\phi+K'_{r\phi\phi}r'\phi^2\\ &-(1+a_H)z'_RF'_N\cos\delta\} \end{aligned}\right\} \quad (3)$$

Definitions of the hydrodynamic derivatives $Y'_v,\ldots Y'_{vvv}$, etc., are widely used nowadays and nearly self-explanatory, but if there is any ambiguity references should be made to the MMG Report[6] and Reference 7 in that order. It should be noted here that the hydrodynamic derivatives $Y'_v,\ldots Y'_{vvv}$, etc., relate only to forces acting upon the naked hull. The forces caused by the rudder are represented by the last term of each formula of Eqs. (3), i.e., $c_{RX}F'_N\sin\delta$, $(1+a_H)F'_N\cos\delta$, etc.

The rudder force F'_N can then be resolved as:

$$F'_N=-\frac{6.13\Lambda}{\Lambda+2.25}\cdot\frac{A_R}{L^2}(u'^2_R+v'^2_R)\sin\alpha_R \quad (4)$$

$$\alpha_R=\delta+\tan^{-1}(v'_R/u'_R) \quad (5)$$

$$u'_R=u'_p\varepsilon\sqrt{1+8kK_T/(\pi J^2)} \quad (6)$$

where

$$J=u'_pV/(nD)$$
$$u'_p=\cos v'[(1-w_p)+\tau\{(v'+x'_pr')^2+c_{pv}v'+c_{pr}r'\}]$$

$$v'_R=\gamma v'+c_{Rr}r'+c_{Rrrr}r'^3+c_{Rrrv}r'^2v' \quad (7)$$

This rather complicated form is taken from the MMG Report[6] and partly from Reference 7. We employ many of the hydrodynamic data from Reference 7 and accordingly follow this form. In the end, however, it is possible to rewrite the whole hydrodynamic forces acting upon the hull and rudder and propeller in the same form as Eqs. (3) but without the F'_N terms. In this case, the hydrodynamic derivatives Y'_v, ... Y'_{vvv}, etc., will change their value to incorporate the rudder force and rudder-hull interference.

3. Test Model and Experimental Results

Table 1 and Fig. 2 illustrate the single-screw container ship we chose for the present study. Since it was originally designed for the SR 108 project by the Japan Shipbuilding Research Association[8], many investigations have been done with this type, including an extensive captive model test for manoeuvrability predictions by Matsumoto and Suemitsu[7].

To their results we have added:

(1) An oblique tow test with various angles of heel to define the sway-roll coupling derivatives.

(2) Measurement of the roll moment exerted by rudder deflection to define the rudder-to-roll coupling derivatives.

Table 1 Principal dimensions of SR 108 container ship

ITEMS				SHIP	MODEL
Hull	Length B. P.	L	(m)	175.00	3.00
	Breadth	B	(m)	25.40	0.435
	Draught Fore	d_F	(m)	8.00	0.1371
	Aft	d_A	(m)	9.00	0.1543
	Mean	d	(m)	8.50	0.1457
	Displacement volume		(m^3)	21,222	0.10686
	Height from keel to transverse metacentre	KM	(m)	10.39	0.1781
	Height from keel to centre of buoyancy	KB	(m)	4.6154	0.07912
	Block coefficient	C_B		0.559	
	Prismatic coef.	C_P		0.580	
	Waterplane area coef.	C_W		0.686	
	Midship section coef.	C_M		0.966	
	L.C.B. from F.P.			0.518 L	
	Radius of gyration about z-axis			0.24 L	
Bilge keel					
	Length		(m)	43.75	0.75
	Depth		(cm)	45.0	0.7714
Rudder	Area	A_R	(m^2)	33.0376	0.009709
	Height	H	(m)	7.7583	0.133
	Aspect ratio	Λ		1.8219	
	Area ratio	A_R/Ld		1/45.0	
Propeller					
	Diameter	D	(m)	6.533	0.112
	Pitch ratio	p		1.009	
	Expanded area ratio			0.67	
	Boss ratio			0.18	
	Number of blades			5	

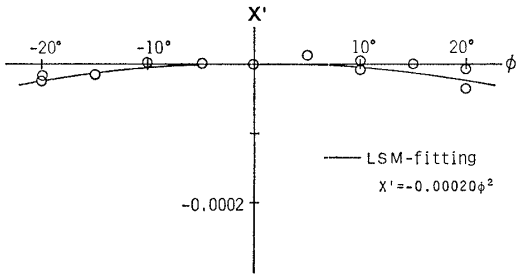

Fig. 3 Longitudinal force coefficient due to roll angle

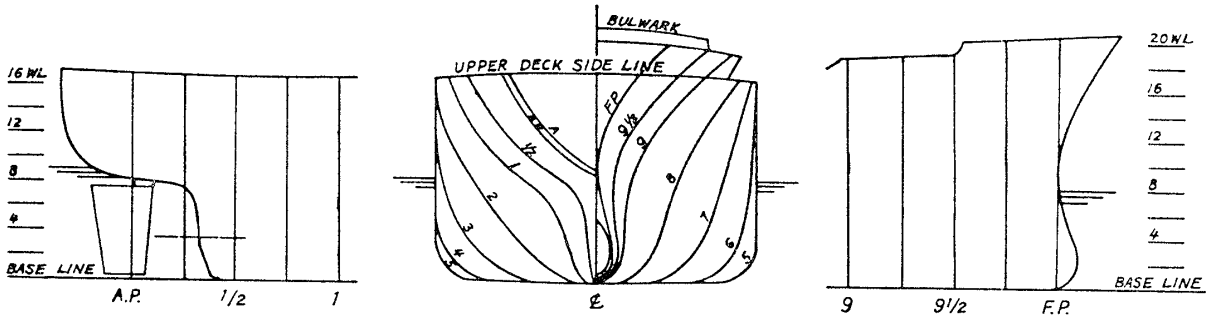

Fig. 2 Lines of SR 108 container ship

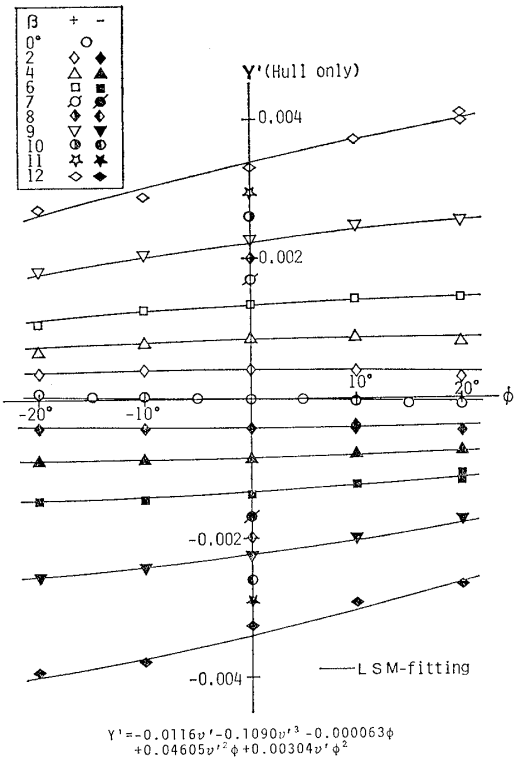

Fig. 4 Lateral force (hull only) coefficient due to roll angle with drift angle

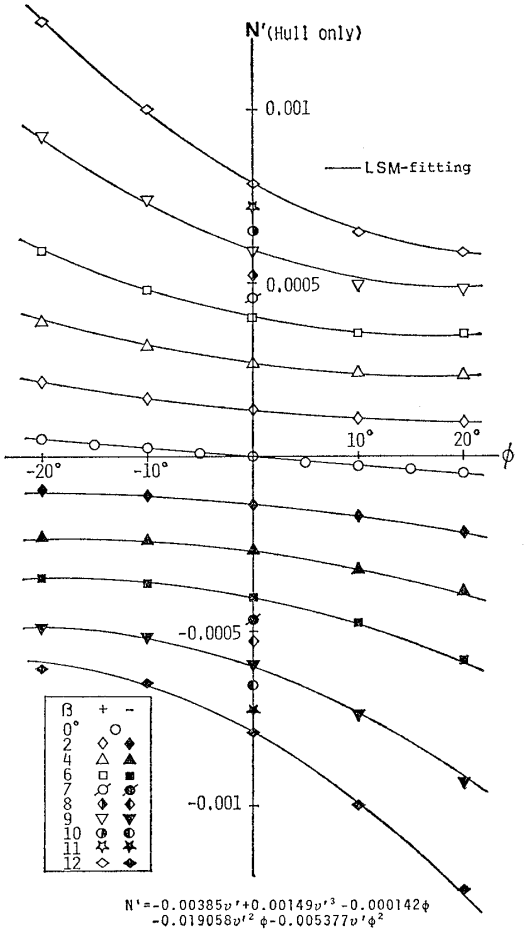

Fig. 5 Yaw moment (hull only) coefficient due to roll angle with drift angle

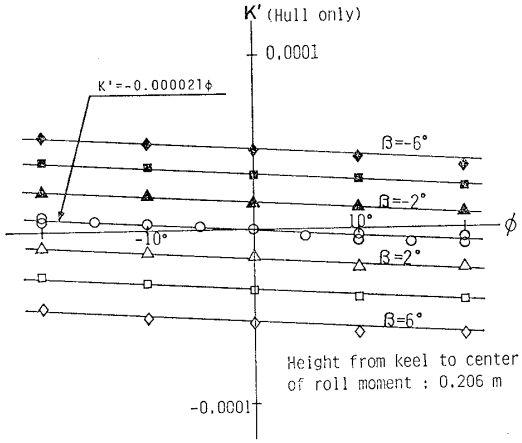

Fig. 6 Roll moment (hull only) coefficient due to roll angle

The oblique tow results are shown in Figs. 3, 4, 5, 6, and 7. Fig. 8 indicates the roll moment versus the lateral force, both of which are exerted by rudder deflection.

The marks in the figures represent the measured data and the curves the least square error fittings. The regression formulae are noted by the figures, where the coefficients define the hydrodynamic derivatives.

Fig. 5 is perhaps particularly interesting among these results for it suggests the key to the roll-to-yaw coupling mechanism. Suppose a ship turning to starboard; she moves obliquely to port and at the same time leans over to port. That means that a ship turning to starboard has a positive β and a negative ϕ (cf. Fig. 1). Fig. 5 indicates that a positive β and a negative ϕ generates a starboard turning moment (positive N'); the greater the heel angle ϕ, the greater the turning moment becomes. Now we can see the sequence: a ship makes turning, she heels over, and the heel generates even greater turning moment. This is a sort of positive feed-back. By this sequence the roll-yaw coupling generally en-

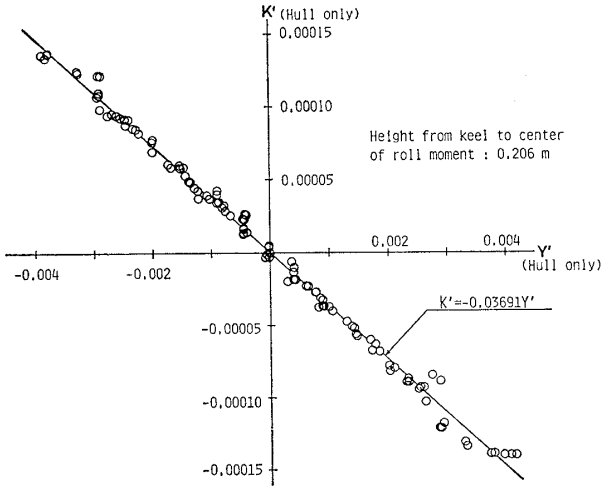

Fig. 7 Relation between K' and Y' (hull only) under oblique running test with heel angle

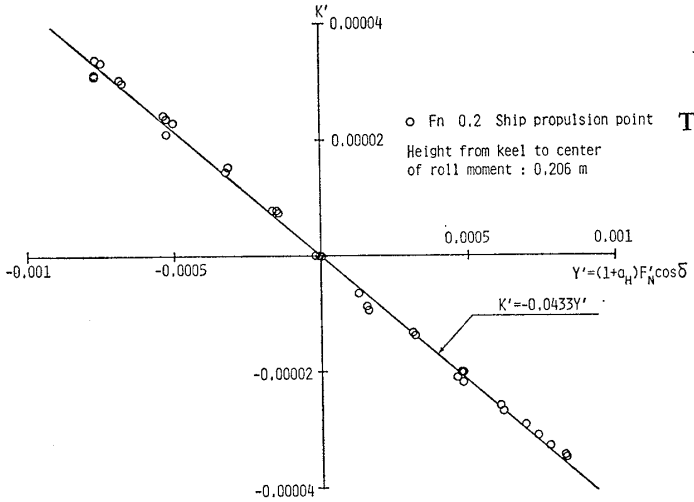

Fig. 8 Relation between K' and Y' induced by rudder deflection on the straight running

courages turning and reduces the effective yaw-damping, thus spoiling the course-stability and quick steering response.

On the basis of these experimental results we have estimated some other derivatives including the yaw-roll coupling ones. The roll damping data of Reference 9 have also been employed.

Eventually we obtain all the necessary derivatives and coefficients as listed in Tables 2 and 3.

Table 2 Hydrodynamic derivatives and coefficients

Yaw moment : Around midship
Roll moment : Around centre of gravity, C.G.
(KG=10.09 m, GM=0.3 m in full size)

a) HULL ONLY

m'	0.00792	$Y'_{\dot{\phi}}$	0.0	$N'_{vv\phi}$	-0.019058
m'_x	0.000238	Y'_{ϕ}	-0.000063	$N'_{\dot{\phi}\phi\phi}$	-0.0053766
m'_y	0.007049	Y'_{vvv}	-0.109	$N'_{rr\phi}$	-0.0038592
I'_x	0.0000176	Y'_{rrr}	0.00177	$N'_{r\phi\phi}$	0.0024195
J'_x	0.0000034	Y'_{rvv}	0.0214	K'_v	0.0003026
I'_z	0.000456	Y'_{rrv}	-0.0405	K'_r	-0.000063
J'_z	0.000419	$Y'_{vv\phi}$	0.04605	K_ϕ	0.1 (Fn≤0.1); 0.2 (Fn≥0.2); Fn (0.1<Fn<0.2)
a'_y	0.05	$Y'_{v\phi\phi}$	0.00304		
l'_x	0.0313	$Y'_{rr\phi}$	0.009325		
l'_y	0.0313	$Y'_{r\phi\phi}$	-0.001368	$K'_{\dot{\phi}}$	-0.000021
K_T	0.527-0.455J	N'_v	-0.0038545	K'_{vvv}	0.002843
X'_{uu}	-0.0004226	N'_r	-0.00222	K'_{rrr}	-0.0000462
X'_{vr}	-0.00311	$N'_{\dot{\phi}}$	0.000213	K'_{rvv}	-0.000558
X'_{vv}	-0.00386	N'_{ϕ}	-0.0001424	K'_{rrv}	0.0010565
X'_{rr}	0.00020	N'_{vvv}	0.001492	$K'_{vv\phi}$	-0.0012012
$X'_{\phi\phi}$	-0.00020	N'_{rrr}	-0.00229	$K'_{v\phi\phi}$	-0.0000793
Y'_v	-0.0116	N'_{rvv}	-0.0424	$K'_{rr\phi}$	-0.000243
Y'_r	0.00242	N'_{rrv}	0.00156	$K'_{r\phi\phi}$	0.00003569

b) PROPELLER AND RUDDER

N_p (rpm)	79.10 (Fn 0.2); 118.64 (Fn 0.3); 158.19 (Fn 0.4)	a_H	0.237	ε	0.921
		x'_H	-0.48	k	0.631
		c_{RX}	0.71	γ	0.088 ($v'>0$); 0.193 ($v'\leq 0$)
$(1-t)$	0.825	z'_R	0.033		
$(1-w_p)$	0.816	c_{pv}	0.0	c_{Rr}	-0.156
x'_R	-0.5	c_{pr}	0.0	c_{Rrrr}	-0.275
x'_p	-0.526	τ	1.09	c_{Rrrv}	1.96

Table 3 Hydrodynamic derivatives around centre of gravity (KG=10.09 m, GM=0.3 m in full size)

HULL PLUS RUDDER

$(m'+m'_y)$	0.01497	$N'_{\dot{\phi}}$	0.000213
$(I'_z+J'_z)$	0.000875	N'_{ϕ}	-0.0001468
$(I'_x+J'_x)$	0.000021	$N'_{vv\phi}$	-0.018191
$m'_y\alpha'$	0.0003525	$N'_{v\phi\phi}$	-0.005299
$m'_y l'_y$	0.0002205	$N'_{rr\phi}$	-0.003684
$Y'_{\dot{v}}$	-0.012035	$N'_{r\phi\phi}$	0.0023843
$(m'+m'_x-Y'_{\dot{r}})$	0.00522	N'_{δ}	0.00126
$Y'_{\dot{\phi}}$	0.0	K_ϕ	0.2
Y'_{ϕ}	-0.0000704	$K'_{\dot{\phi}}$	-0.000021
$Y'_{vv\phi}$	0.046364	K'_v	0.000314
$Y'_{v\phi\phi}$	0.003005	$(m'_x l'_x+K'_{\dot{r}})$	-0.0000692
$Y'_{rr\phi}$	0.0093887	$K'_{vv\phi}$	-0.0012094
$Y'_{r\phi\phi}$	-0.0013523	$K'_{v\phi\phi}$	-0.0000784
Y'_{δ}	-0.002578	$K'_{rr\phi}$	-0.0002449
$N'_{\dot{r}}$	-0.00243	$K'_{r\phi\phi}$	0.00003528
$N'_{\dot{v}}$	-0.0038436	K'_{δ}	0.0000855

4. Manoeuvring Prediction Taking Roll Coupling into Account

Solving Eqs. (2) and (3) with the numerical data from Tables 2 and 3 makes it possible to predict the ship motion induced by any given rudder execution.

Fig. 9 illustrates the turning paths and accompanying roll angle time histories with a rudder deflection of 15°. The smaller metacentric height (GM) naturally results in the greater roll angle with the same rudder deflec-

tion; this in turn makes the hydrodynamic yaw damping the less and thus turning path becomes the tighter.

A similar trend is also seen in zig-zag manoeuvre shown in Fig. 10: the roll coupling makes a ship less stable on course and slower in response.

In both cases the effect of the roll coupling can be considerable. This is especially true when the metacentric heihgt is small.

5. Unstable Behaviour Induced by Yaw-Sway-Roll-Rudder Coupling

We have already pointed out the unstable character of the roll-yaw coupling: once given a yaw motion, the yaw induces roll and the roll accelerates yaw even more. Together with the rudder movement in accordance with yaw motion, this unstable character can generate a self-exciting, roll-yaw coupling oscillation of an automatically steered ship. Because it is of a self-exciting type, this oscillation can become really wild.

Taggart[1] suggested this type of yaw-induced roll as early as 1970 and recently Eda[2] carried out a digital simulation study based on captive model tests to indicate the feasibility of this kind of coupling oscillation.

We will perform in this section a mathematical analysis of this yaw-roll-rudder coupling instability on the basis of Eqs. (2) and (3) and the captive model data, both of which were already introduced in the previous sections.

5.1 Equations of Motion

Suppose a ship sailing nearly straight with an automatic course-keeping device in operation. We can assume a constant ship speed, so the first equation of Eqs. (2), the surge equation, can be omitted.

Among hydrodynamic derivatives, the third-order terms of yaw and sway can be omitted because yaw and sway velocities remain rather small in the situation under consideration. The terms $m'_y\alpha'_y\dot{r}'$ and $m'_y\alpha'_y\dot{v}'$ are generally so small that they can also be omitted.

The higher-order terms of yaw-roll and

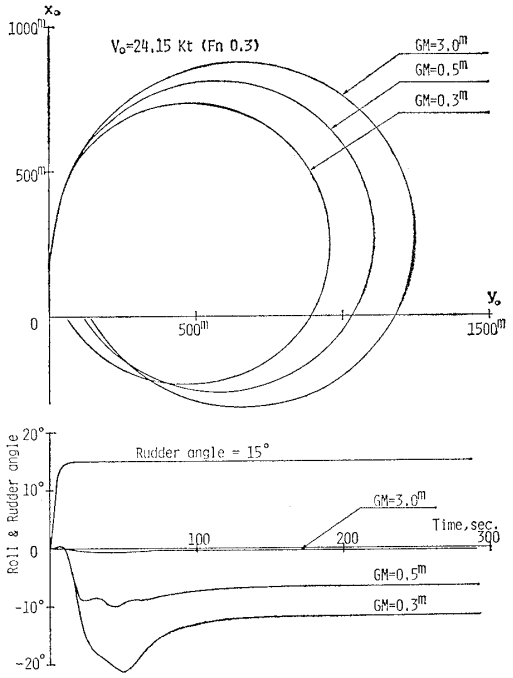

Fig. 9 Turning trajectory and roll angle

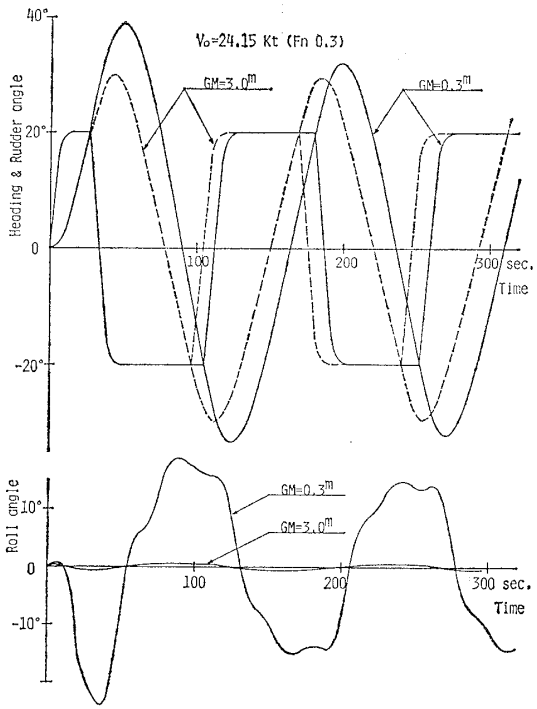

Fig. 10 Z-Manoeuvre response and roll angle

sway-roll coupling, however, should be included. This is because:

(1) The roll angle may well reach 20°, which can hardly be considered small.

(2) As is indicated in Fig. 5, even a rather small sway velocity does accelerate the roll-yaw coupling considerably, which implies a significant contribution of higher-order coupling terms.

The equations of motion for the analysis of this section then become:

$$\left.\begin{aligned}
&(m'+m_y')\dot{v}'-Y_v'v'+(m'+m_x'-Y_r')r'\\
&\quad -m_y'l_y'\dot{p}'-Y_{\dot{\phi}}'p'-Y_\phi'\phi-Y_{vv\phi}'v'^2\phi\\
&\quad -Y_{v\phi\phi}'v'\phi^2-Y_{rr\phi}'r'^2\phi-Y_{r\phi\phi}'r'\phi^2\\
&\quad =Y_\delta'\delta\\
&(I_z'+J_z')\dot{r}'-N_r'r'-N_v'v'-N_{\dot{\phi}}'p'-N_\phi'\phi\\
&\quad -N_{vv\phi}'v'^2\phi-N_{v\phi\phi}'v'\phi^2-N_{rr\phi}'r'^2\phi\\
&\quad -N_{r\phi\phi}'r'\phi^2=N_\delta'\delta\\
&(I_x'+J_x')\dot{p}'-K_{\dot{\phi}}'p'+(W'GM'-K_\phi')\phi\\
&\quad -m_y'l_y'\dot{v}'-K_v'v'-(m_x'l_x'+K_r')r'\\
&\quad -K_{vv\phi}'v'^2\phi-K_{v\phi\phi}'v'\phi^2-K_{rr\phi}'r'^2\phi\\
&\quad -K_{r\phi\phi}'r'\phi^2=K_\delta'\delta\\
&\text{where}\quad p'=\dot{\phi}'=\dot{\phi}(L/V)
\end{aligned}\right\} \tag{8}$$

Next we will assume a proportional-and-derivative control auto-pilot and a steering gear with an exponential lag. The latter is a good approximation of current electro-hydraulic steering gears.

The equation of this rudder control mechanism is:

$$T_E'\dot{\delta}'+\delta=-a\phi-b'\dot{\phi}' \tag{9}$$

where $\dot{\phi}'=\dot{\phi}(L/V)=r'$, $b'=b(V/L)$, and where $T_E'=T_E(V/L)$, T_E being the time constant of the steering gear, and a and b denote the "proportional" and "derivative" control parameters, respectively, of the auto-pilot.

Eqs. (8) and (9) compose the set of simultaneous differential equations which the present analysis is based upon.

5.2 Stability Analysis—Root Locus and Range of Stability Diagrams

When the yaw and sway velocities and the roll angle are all very small, the stability analysis is simple: the third-order terms of the roll-yaw and roll-sway coupling can then be omitted and Eqs. (8) become linear. We can define the characteristic roots, or eigen-values, which govern the stability.

The results are indicated in Figs. (11) and (12) by the ×-marks. There are six eigen-values and all the real parts of them are negative in these two cases. The whole system (ship and rudder control device) is then stable, and any small deviation from upright ($\phi=0$), straight sailing ($r'=v'=0$) will decay out with time.

Next we will consider the case when the yaw, sway, and roll are not very small. The third-order coupling terms can not be omitted, then. We will employ the principle of perturbation stability around an arbitrary equilibrium situation.

Assuming an equilibrium of $r'=r_0'$, $v'=v_0'$, and $\phi=\phi_0$, a small perturbation around it is described by the following equations:

$$\left.\begin{aligned}
&(m'+m_y')\dot{v}'-Y_2v'+Y_3r'-Y_4\dot{p}'\\
&\quad -Y_5p'-Y_6\phi=Y_\delta'\delta\\
&(I_z'+J_z')\dot{r}'-N_2r'-N_3v'-N_4p'\\
&\quad -N_5\phi=N_\delta'\delta\\
&(I_x'+J_x')\dot{p}'-K_2p'+K_3\phi-K_4\dot{v}'\\
&\quad -K_5v'-K_6r'=K_\delta'\delta\\
&T_E'\dot{\delta}+\delta=-a\phi-b'\dot{\phi}'
\end{aligned}\right\} \tag{10}$$

It should be here noted, however, that all the motion parameters v', r', ϕ, δ, in this equation are ones of small perturbation, not the whole amount of the motion parameters. For example, whole sway velocity is v_0+v, v being the perturbation. The new coefficients Y's, N's, and K's are:

$$\left.\begin{aligned}
&Y_2=Y_v'+2Y_{vv\phi}'v_0'\phi_0+Y_{v\phi\phi}'\phi_0^2\\
&Y_3=(m'+m_x'-Y_r')-2Y_{rr\phi}'r_0'\phi_0-Y_{r\phi\phi}'\phi_0^2
\end{aligned}\right|$$

$$
\begin{aligned}
Y_4&=m'_y l'_y\\
Y_5&=Y_{\dot\phi}'\\
Y_6&=Y'_\phi+Y'_{vv\phi}v'^2_0+2Y'_{v\phi\phi}v'_0\phi_0+Y'_{rr\phi}r'^2_0\\
&\quad+2Y'_{r\phi\phi}r'_0\phi_0\\
N_2&=N'_r+2N'_{rr\phi}r'_0\phi_0+N'_{r\phi\phi}\phi_0^2\\
N_3&=N'_v+2N'_{vv\phi}v'_0\phi_0+N'_{v\phi\phi}\phi_0^2\\
N_4&=N_{\dot\phi}'\\
N_5&=N'_\phi+N'_{vv\phi}v'^2_0+2N'_{v\phi\phi}v'_0\phi_0+N'_{rr\phi}r'^2_0\\
&\quad+2N'_{r\phi\phi}r'_0\phi_0\\
K_2&=K_{\dot\phi}'\\
K_3&=(\mathrm{W'GM'}-K'_\phi)-K'_{vv\phi}v'^2_0-2K'_{v\phi\phi}v'_0\phi_0\\
&\quad-K'_{rr\phi}r'^2_0-2K'_{r\phi\phi}r'_0\phi_0\\
K_4&=m'_y l'_y\\
K_5&=K'_v+2K'_{vv\phi}v'_0\phi_0+K'_{v\phi\phi}\phi_0^2\\
K_6&=(m'_x l'_x+K'_r)+2K'_{rr\phi}r'_0\phi_0+K'_{r\phi\phi}\phi_0^2
\end{aligned}
\qquad (11)
$$

Eqs. (10) are obviously linear, and therefore the stability of small perturbation around the situation v'_0, r'_0, and ϕ_0 can be examined by the same procedure already mentioned in the stability analysis for upright, straight sailing.

The algebraic equation to define the eigenvalues is

$$\lambda^6+A_1\lambda^5+A_2\lambda^4+A_3\lambda^3+A_4\lambda^2+A_5\lambda+A_6=0 \qquad (12)$$

where A's are composed of the coefficients of Eqs. (10).

Eqs. (11) tell us that the coefficients Y's, N's, and K's do change their values with the initial motion v'_0, r'_0, and ϕ_0, so the same is true of the A's of Eq. (12). The stability eigenvalues thus change with the initial motion v'_0, r'_0, and ϕ_0.

Figs. 11 and 12 illustrate this. Starting at the ×-mark that corresponds to straight sailing, the characteristic roots move along the arrow-headed solid curves with increasing initial yaw velocity r'_0. In this figure, the initial sway velocity is given to be proportional to r'_0, i.e.:

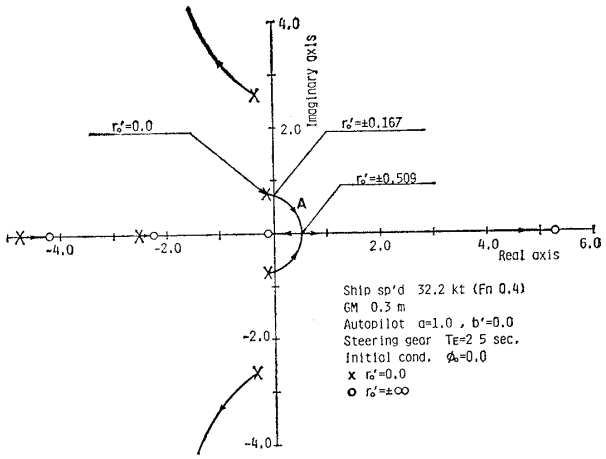

Fig. 11 Root locus diagram of stability characteristic equation; $\phi_0=0$, without yaw-rate control

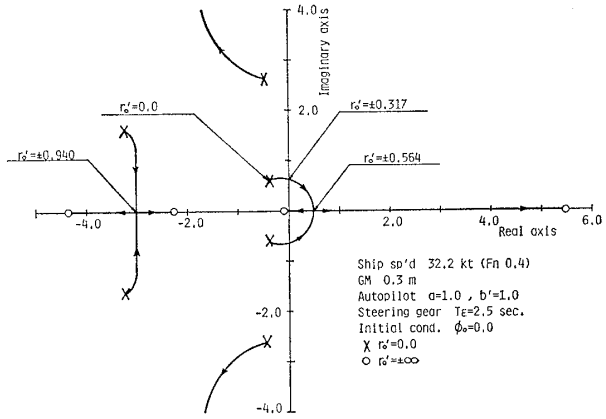

Fig. 12 Root locus diagram of stability characteristic equation; $\phi_0=0$, yaw-rate gain $b'=1.0$

$$v'_0=-0.45r'_0 \qquad (13)$$

This means that the pivoting point is located 0.45 ship length in front of C.G.

According to Fig. 11, the ship is stable at upright and straight sailing because all the roots remain on the left-half plane. Any small rolling will decay with time. With increasing yaw velocity r'_0, however, a pair of complex roots move to rightward and cross over the imaginary axis when r'_0 reaches ±0.167. This means that the ship (and the whole system) becomes unstable when her yaw velocity exceeds 0.167. Now any small rolling will build up and the ship develops heavy rolling accompanied by considerable zig-zag yawing

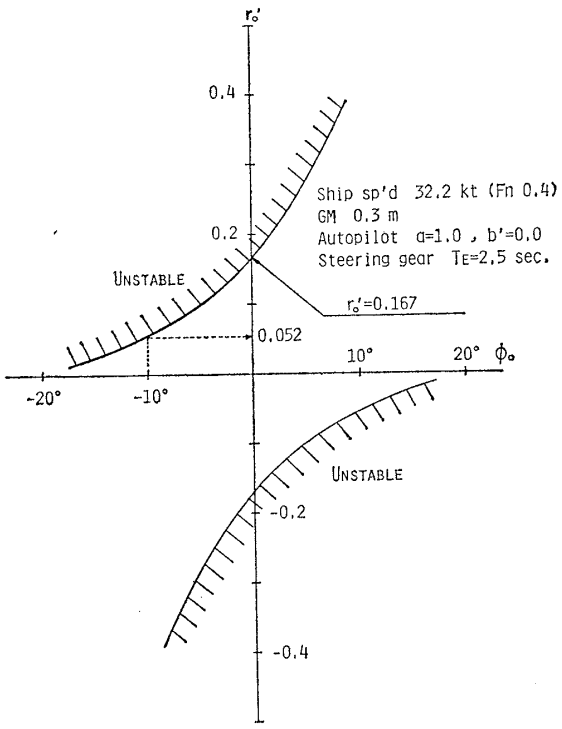

Fig. 13 Stability region as a function of initial motions, r_0' and ϕ_0; without yaw-rate control

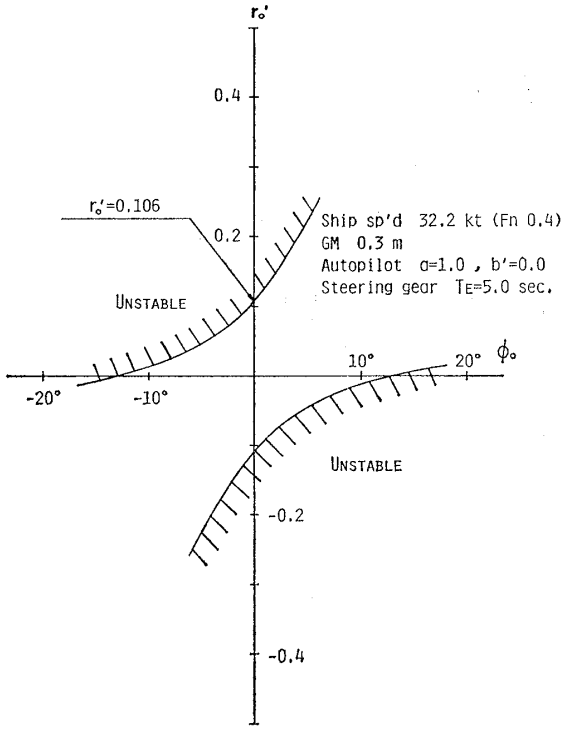

Fig. 15 Stability region as a function of initial motions, r_0' and ϕ_0; slow steering gear speed

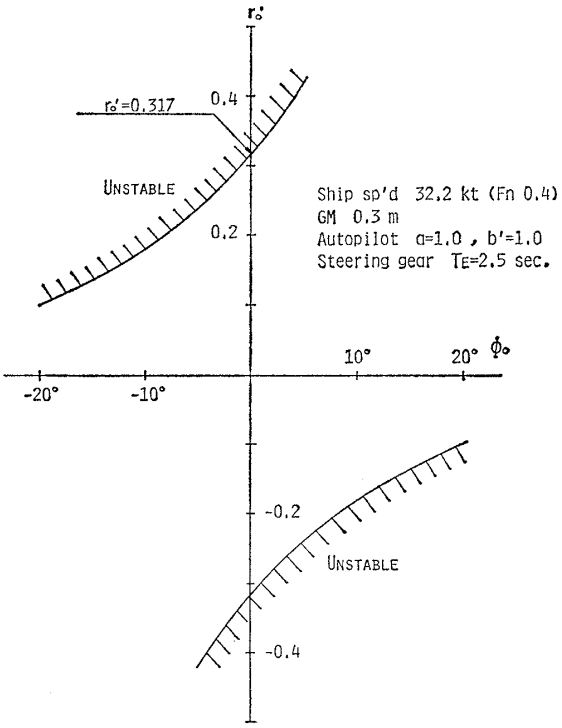

Fig. 14 Stability region as a function of initial motions, r_0' and ϕ_0; yaw-rate gain $b'=1.0$

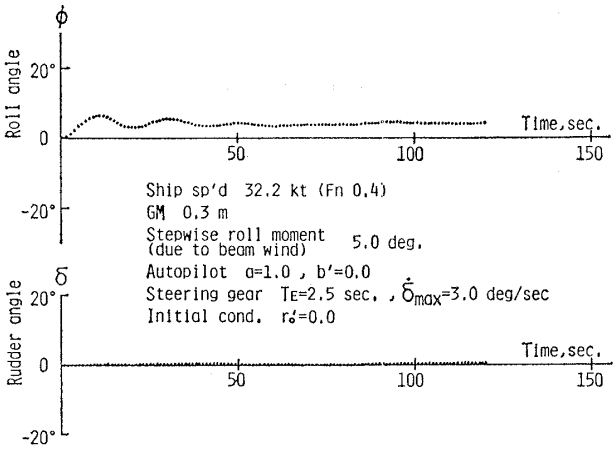

Fig. 16 Roll-yaw-rudder coupled motion with autopilot; without initial yaw motion and without yaw-rate control

(cf. Fig. 17).

This is visualized in Figs. 16 and 17. We solved Eqs. (8) and (9) numerically, giving an initial yaw rate of 0.0 and 0.16, respectively, and a small stepwise roll moment. Without initial yaw velocity the whole system is stable (Fig. 16), but with r_0'=0.16, the system gets into

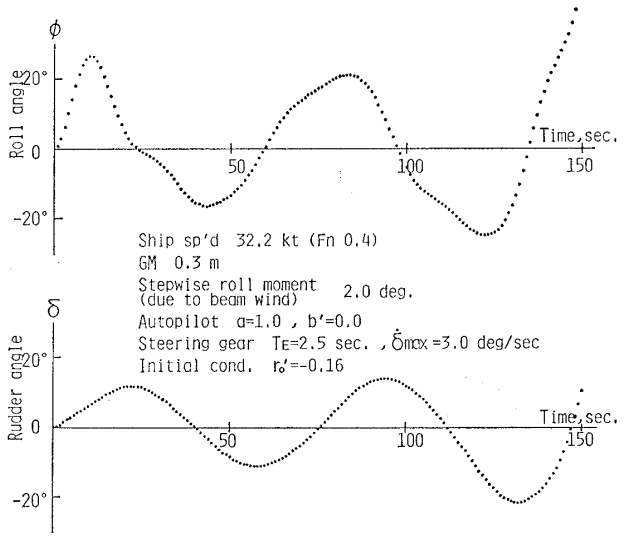

Fig. 17 Roll-yaw-rudder coupled motion with auto-pilot; initial yaw-rate $r_0' = -0.16$ and without yaw-rate control

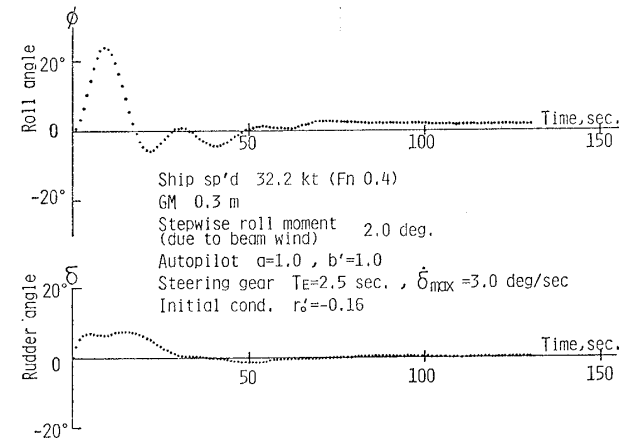

Fig. 18 Roll-yaw-rudder coupled motion with auto-pilot; initial yaw-rate $r_0' = -0.16$ but with yaw-rate control

a self-exciting, diverging oscillation (Fig. 17). The period is about 80 sec., which is much longer than the natural period of rolling, 30 sec.

Fig. 11 corresponds to the case of no roll angle, i.e., upright. We can draw a similar root locus diagram with a certain amount of roll angle, ϕ_0, with changing r_0'. The result tells us that the greater the initial heel ϕ_0 to outward, the smaller becomes the critical r_0' at which the whole system gets unstable. Outward heel means to lean over to the opposite side of turning, i.e., opposite signs between yaw and roll.

Fig. 13 illustrates this. The ordinate is the initial yaw velocity r_0' (non-dimensional), and the abscissa the initial heel angle, ϕ_0. The curves indicate the boarder-line stability. Without any initial heel the critical (boarder-line) r_0' is ± 0.167, as is shown by Fig. 11. With an initial heel of 10° to *port* (negative ϕ) for example, a much smaller initial *starboard* turning, $r_0' = +0.052$ becomes critical. The destabilizing effect of an outward heel is quite obvious.

On the contrary, an inward heel is much safer than an outward one. The captive model experimental data of Fig. 5 tells us the basic reason for this. Incidentally, Fig. 13 also shows that a heel angle of about 20° may induce unstable motion without any initial yaw motion.

In the case of Fig. 13, the derivative control, or yaw-rate gain of the auto-pilot, is zero ($b'=0$). Introducing the yaw-rate control improves the stability of the whole system significantly, as is illustrated by Fig. 14. This is also confirmed by the digital simulation results of Fig. 18. It may be rather surprising to see how effective the yaw-rate auto-pilot is in suppressing heavy rolling which would otherwise exist, in spite of the fact that it has no direct action against rolling. This is a very interesting point of the yaw-roll coupling.

Fig. 15 displays the effect of the steering gear speed on the stability of the whole system. In this case the steering gear time constant is doubled, that means the steering gear speed is halved. The effect is considerable: the critical yaw-rate at upright sailing lessens to 0.106 and the critical roll angle at straight sailing becomes as small as about 10°. Again it is interesting that the steering gear speed has a great influence on rolling at sea. Together with the previous results for the auto-pilot yaw-rate control, this reminds us of a common belief among small boat skippers that skillful

steering is essential to avoid heavy rolling at sea.

6. Conclusions

The important conclusions we obtained are:

(1) The captive model tank tests revealed that yaw moment and sway force induced by roll depend much upon the yaw and sway velocities. This is particularly true for an *outward* heel, the lean over to the opposite side of the ship's turning. Accordingly the yaw-roll and sway-roll coupling hydrodynamic forces have essentially a non-linear character. The third-order, cross-coupling hydrodynamic derivatives play an important roll as well as the linear terms in the mathematical modelling of the hydrodynamic forces acting upon a hull.

(2) The yaw-sway-roll coupling has a destabilizing effect on the yaw motion of a ship: improving turning performance and spoiling directional stability and quick response. The smaller the metacentric height and the higher the ship speed, the more prominent this tendency becomes.

(3) The yaw-sway-roll coupling can induce a self-exciting, heavy rolling accompanied by a considerable yawing of a ship under automatic course-keeping. Since this phenomenon depends much upon the higher-order yaw-roll cross-coupling, an accidental heel over of moderate degree will not last long if a ship is sailing really straight. Once she begins to yaw and sway, however, even an infinitesimally small heel can develop into heavy rolling accompanied by yawing.

(4) The performance of an auto-pilot has a great effect on this unstable behaviour. Yaw-rate control proved very effective in suppressing this type of heavy yaw-roll motion. Slowing down the steering gear speed spoils the overall stability considerably.

Acknowledgement

Acknowledgement is made to Prof. H. Eda of Davidson Laboratory as well as to Prof. M. Hamamoto of Osaka University for their influential discussions and valuable advice. We are also indebted to Mr. H. Tatano and the staff of the Manoeuvrability Laboratory of Osaka University for their help at experimental tank.

References

1) R. TAGGART: Anomalous Behavior of Merchant Ship Steering Systems, Marine Technology, Vol. 7, No. 2 (1970)
2) H. EDA: Rolling and Steering Performance of High Speed Ships, 13th O.N.R. Symposium (1980)
3) M. HIRANO and J. TAKASHINA: A Calculation of Ship Turning Motion Taking Coupling Effect Due to Heel into Consideration, Trans. of West-Japan S.N.A., No. 59 (1980)
4) J. N. NEWMAN: Marine Hydrodynamics, MIT Press, 1978
5) J. STRØM-TEJSEN: A Digital Computer Technique for Prediction of Standard Maneuvers of Surface Ships, DTMB Report No. 2130 (1965)
6) A. OGAWA, K. HASEGAWA and Y. YOSHIMURA: MMG Report V—On the Experimental Verification and Improvement of Mathematical Modeling for Manoeuvring Motions, Bulletin of S.N.A. of Japan, No. 616 (1980) (in Japanese)
7) N. MATSUMOTO and K. SUEMITSU: The Prediction of Manoeuvring Performances by Captive Model Tests, J. of Kansai S.N.A., Japan, No. 176 (1980) (in Japanese)
8) SR 125: Research on Seakeeping Performances of Super-High-Speed Container Ships, SR Report No. 211, 1975 (in Japanese)
9) N. TANAKA, Y. HIMENO, M. OGURA and K. MASUYAMA: Free Rolling Test at Forward Speed, J. of Kansai S.N.A., Japan, No. 146 (1972) (in Japanese)
10) Kansai S.N.A., Japan: Handbook of Ship Design, Kaibundo, 1961 (in Japanese)
11) 15th ITTC Proceedings: Report of Performance Committee, 1978
12) N. MATSUMOTO and K. SUEMITSU: Manoeuvring Performance Test Analysis by Mathematical Response Model, J. of Kansai S.N.A., Japan, No. 180 (1981) (in Japanese)